

Original Article

MeCP2 gene therapy ameliorates disease phenotype in mouse model for Pitt Hopkins syndrome

Cassandra N. Dennys^a, Sheryl Anne D. Vermudez^b, Robert J.M. Deacon^c,
J. Andrea Sierra-Delgado^a, Kelly Rich^a, Xiaojin Zhang^a, Aditi Buch^b, Kelly Weiss^b,
Yuta Moxley^b, Hemangi Rajpal^b, Francisca D. Espinoza^d, Samantha Powers^a, Ariel S. Ávila^d,
Rocco G. Gogliotti^e, Patricia Cogram^c, Colleen M. Niswender^{b,f,g,h}, Kathrin C. Meyer^{a,i,j,*}

^a Center for Gene Therapy, The Abigail Wexner Research Institute at Nationwide Children's Hospital, Columbus, OH, USA

^b Department of Pharmacology and Warren Center for Neuroscience Drug Discovery, Vanderbilt University, Nashville, TN 37232, USA

^c Department of Genetics, Institute of Ecology and Biodiversity, Faculty of Science, University of Chile, Chile

^d Faculty of Medicine, Universidad Católica de la Santísima Concepción, Concepción, 4090541, Chile

^e Department of Molecular Pharmacology and Neuroscience, Loyola University Chicago, Maywood, IL 60153, USA

^f Vanderbilt Institute of Chemical Biology, Vanderbilt University, Nashville, TN 37232, USA

^g Vanderbilt Brain Institute, Vanderbilt University, Nashville, TN 37232, USA

^h Vanderbilt Kennedy Center, Vanderbilt University Medical Center, Nashville, TN 37232, USA

ⁱ Department of Pediatrics, The Ohio State University Medical Center, Columbus, OH, USA

^j Department of Neuroscience, The Ohio State University Wexner Medical Center, Columbus, OH, USA

ARTICLE INFO

Keywords:

Pitt Hopkins syndrome

TCF4

AAV gene therapy

MeCP2

ABSTRACT

The neurodevelopmental disorder Pitt Hopkins syndrome (PTHS) causes clinical symptoms similar to Rett syndrome (RTT) patients. However, RTT is caused by *MECP2* mutations whereas mutations in the *TCF4* gene lead to PTHS. The mechanistic commonalities underlying these two disorders are unknown, but their shared symptomatology suggest that convergent pathway-level disruption likely exists. We reprogrammed patient skin derived fibroblasts into induced neuronal progenitor cells. Interestingly, we discovered that MeCP2 levels were decreased in PTHS patient iNPCs relative to healthy controls and that both iNPCs and iAstrocytes displayed defects in function and differentiation in a mutation-specific manner. When *Tcf4*^{+/-} mice were genetically crossed with mice overexpressing MeCP2, molecular and phenotypic defects were significantly ameliorated, underlining and important role of MeCP2 in PTHS pathology. Importantly, post-natal intracerebroventricular gene replacement therapy with adeno-associated viral vector serotype 9 (AAV9)-expressing MeCP2 (AAV9.P546.MeCP2) significantly improved iNPC and iAstrocyte function and effectively ameliorated histological and behavioral defects in *Tcf4*^{+/-} mice. Combined, our data suggest a previously unknown role of MeCP2 in PTHS pathology and common pathways that might be affected in multiple neurodevelopmental disorders. Our work highlights potential novel therapeutic targets for PTHS, including upregulation of MeCP2 expression or its downstream targets or, potentially, MeCP2-based gene therapy.

Introduction

Pitt-Hopkins syndrome (PTHS) is a rare neurodevelopmental disorder that is characterized by moderate to severe intellectual disability, global developmental delay, dysmorphic facial features, and episodic hyperventilation followed by periods of apnea [1]. Many individuals with PTHS are nonverbal, and exhibit symptoms of autism spectrum disorder, stereotypic hand movements, seizures, and sleep

disturbances [2]. Typical onset occurs in infancy, with diagnosis established via genetic testing to confirm a mutation in the *Transcription Factor 4* (*TCF4*) gene [3]. PTHS is the result of *TCF4* haploinsufficiency, arising from either a pathogenic variant in, or deletion of, the genomic region which encompasses *TCF4* (18q21.2). Currently, treatment of PTHS is entirely focused on managing symptoms – there are no therapies that target the underlying molecular pathology of the disease.

* Corresponding author.

E-mail address: km2dq@missouri.edu (K.C. Meyer).

<https://doi.org/10.1016/j.neurot.2024.e00376>

Received 17 October 2023; Received in revised form 7 May 2024; Accepted 14 May 2024

1878-7479/© 2024 Published by Elsevier Inc. on behalf of American Society for Experimental NeuroTherapeutics. This is an open access article under the CC BY-NC-ND license (<http://creativecommons.org/licenses/by-nc-nd/4.0/>).

The size of the *TCF4* gene (360 kb) and its vast number of isoforms make the development of classical gene replacement therapy difficult. There are no capsids with large enough carrying capacity for the entire gene, thus restricting gene therapy to the use of a single coding sequence for the most frequent isoform [4]. At present, it is unclear if such an approach would provide an optimal therapeutic outcome. Gene-agnostic or gene-independent therapies that target specific dysregulated molecular pathways may also provide clinical benefit to patients with neurodevelopmental disease regardless of genetic cause.

Interestingly, PTHS clinical symptoms overlap with that of other developmental diseases, including Rett syndrome (RTT, [2]), for which several gene replacement strategies are currently being tested in the clinic and for which the FDA recently approved Trofinetide (Daybue®) as a novel small molecule therapeutic (NCT05898620, NCT05606614). RTT is an X-linked developmental disorder caused by mutations in the *Methyl CpG Binding Protein 2 (MECP2)* gene leading to protein loss-of-function ([5,6] reviewed in Refs. [7–9]). The clinical manifestation of RTT parallels PTHS to such a high degree that it is often one of the first differential diagnoses for PTHS patients before genetic testing [2]. Such extensive clinical overlap suggests potential common disease pathways which could be exploited therapeutically.

We discovered functional deficits in reprogrammed induced neuronal progenitor cells (iNPCs) and induced astrocytes (iAs) from PTHS patients in conjunction with reduced MeCP2 protein levels. These findings were then confirmed in brain tissue of 60-day old *Tcf4*^{+/-} heterozygous mice. Crossing the *Tcf4*^{+/-} heterozygous mouse with a mouse model that overexpresses MeCP2 normalized molecular and behavioral pathologies to a level comparable to healthy controls, confirming the important role of MeCP2 in PTHS disease manifestation. Importantly, treatment of patient-derived iNPCs and astrocytes, as well as *Tcf4*^{+/-} heterozygous mice, with an adeno-associated viral vector serotype 9 (AAV9) expressing MeCP2 (AAV9.P546.MeCP2) improved cellular function and restored histological and behavioral deficits.

Taken together, these results provide compelling evidence for an important role of MeCP2 in PTHS pathology and open new potential therapeutic avenues based on genetic and non-genetic therapies currently in development for RTT.

Methods

Cell Culture: Cells were obtained from human skin and all subjects gave their consent to the study in accordance with the informed consent regulations of the institution where the research was conducted. PTHS patient fibroblasts were converted to neuronal progenitor cells as previously described [10–12]. Neuronal progenitor cells were cultured on fibronectin-coated dishes in NPC media (DMEM/F12 media containing 1% N2 supplement [Life Technologies], 1% B27 and 20 ng/ml fibroblast growth factor-2) until confluent. At this time, cells were either lifted and pelleted for western analysis or differentiated into astrocytes using astrocyte-inducing media (DMEM media containing 10% FBS and 0.2% N2) as previously described [10]. For AAV9 treatment, we used a modified version of a previously published protocol [54]. Briefly, NPCs were treated with neuraminidase (NA) for 2 h in suspension. After NA treatment, cells were seeded according to the regular NPC protocol and transduced with scAAV9.546.MeCP2 at a Multiplicity of Infection (MOI) of 100,000 K. Two days following transduction, cells were lifted and differentiated into astrocytes for 5 days.

Co-culture: Stem cells from HB9:GFP+ mouse embryos were cultured as described previously [10,12,13]. Embryonic bodies (EB) were cultured in EB differentiation media (knockout DMEM/F12, 10% knockout serum replacement, 1% N2, 0.5% L-glutamine, 15% glucose, and 0.008% 2-mercaptoethanol) with smoothed agonist (SAG) and 2 μ M retinoic acid freshly added starting day 2 of differentiation. EBs were dissociated as previously described [12] and sorted using BD (Becton-Dickenson) Influx sorter running Sortware software. Cells were sorted through a 100- μ m tip at a sheath pressure of 27.5. Following sorting, GFP+ neurons

were seeded in a 96 well plate (10,000 cells per well). Cells were cultured in motor neuron media (DMEM/F12, 5% horse serum, 2% N2, 2% B27 supplemented with 10 ng/mL of each GDNF, BDNF, CNTF) for up to four days. The entire well was imaged using the InCell 6000 plate reader and analysis was conducted on the entire field of view. Survival, skeletal length and average neurite length were quantified using the InCell Developer and Analyzer.

Animal Housing: All animals used in the present study were group housed with food and water given ad libitum and maintained on a 12 h light/dark cycle with room temperature (21 \pm 2 °C), relative humidity (55 \pm 5%), a 12-h light–dark cycle (lights on 7 a.m.–7 p.m.) and air exchange (16 times per h) automatically controlled. Animals were cared for in accordance with the National Institutes of Health Guide for the Care and Use of Laboratory Animals. Mice used for behavioral experiments were different from those utilized for molecular assays.

Animals utilized for cross breeding experiments (Vanderbilt University): All studies were approved by the Institutional Animal Care and Use Committee for Vanderbilt University School of Medicine and took place during the light phase. *Tcf4* \pm mice were cryo recovered from The Jackson Laboratory (B6; 129-Tcf4tm1Zhu/J, stock no. 013598), and maintained by breeding male *Tcf4* \pm with female WT C57BL/6Jx129S F1 hybrid mice (The Jackson Laboratory, B6129SF1/J, stock no. 101043). *MECP2*Tg1/o mice (C57BL/6J background) were generously shared by Dr. Jeffrey Neul (Vanderbilt University Medical Center). Experimental mice were obtained by crossing *Tcf4* \pm and *MECP2*Tg1/o mice. Male mice were aged until the predicted symptomatic age of 20 weeks old for all experiments.

Animals used for injection (University of Chile): Heterozygous male B6; 129-Tcf4tm1Zhu/J mice acquired from the Jackson Laboratory (stock #013598) and bred with female B6129SF1/J mice (stock #101043) to produce *Tcf4* \pm and *Tcf4*+/+ littermates. Genotyping of transgenic mouse line B6; 129-Tcf4tm1Zhu/J originated from the Jackson Laboratory was done according to Jackson Laboratory guidelines using PCR with the following primers: FW: 5'-AGCGCGA-GAAAGGAACGGAGGA-3', RV1 5' GGCAATTCTCGGGAGGGTGCTT-3', and RV2 5'-CCAGAAAGCGAAGGAGCA-3' (expected product 229 bp for WT allele and 400 bp for KO allele). Intracerebroventricular (ICV) injections were performed on P1 (first day of life) mice using Hamilton Syringes (Catalog No. 80330 700RN 10 μ L SYR (26s/2'')/2) REV M Lot #324603 11/08/2005) with Hamilton needles (Catalog No. 7803-05 NDL. NDL 6pk 33 GA RN 75"20 DEG PT S/0# 83521 02/17/2005) as previously published (JOVE article with a video: "Delivery of Therapeutic Agents Through Intracerebroventricular (ICV) and Intravenous (IV) Injection in Mice"). Each pup was transcranially injected with 1.5x10¹⁰ vgs at p1, returned to the mother and genotyped at P15 using TransnetXY Automated Genotyping. Behavioral testing was performed blinded on *Tcf4* \pm and *Tcf4*+/+ male mice the animals reached P60.

Cross Bred Animal Behavioral Assays (Vanderbilt University): All behavioral experiments were conducted from the predicted symptomatic age (20–26 weeks) at the Vanderbilt Neurobehavioral Core. Male mice were used and open field and elevated zero maze were conducted in the same cohort of mice with a minimum of 3 days between each assay. For each assay, mice were habituated to the testing room for 1 h prior to the experiment. Quantification was performed either by a researcher blinded to the genotype or by automated software.

Open Field: Male mice were placed in an activity chamber for 1 h and locomotor and vertical activities were quantified as beam breaks in the X, Y and Z axis using Activity Monitor software (Med Associates Inc, St. Albans, VT, USA).

Elevated Zero Maze: The elevated plus maze has two open arms and two closed arms; all arms are 20 cm in length and 8 cm in width. The maze is elevated 50 cm above the floor. Mice were placed on a continuous circular platform with two closed and two open regions for 5 min under full light conditions (~700 lux in the open regions, ~400 lux in the closed regions). For cross bred animals, the time spent exploring the open regions were quantified by ANY-maze software (Stoelting, Wood Dale, IL, USA).

Injected Animal Behavioral Assays (University of Chile): All behavioral experiments were conducted on 15 male mice at p60 days. For each assay, mice were habituated to the testing room for 1 h prior to the experiment. Quantification was performed either by a researcher blinded to the genotype or by automated software.

Open Field: Mice were given 30 min to habituate followed by a 30 min trial. The total distance travelled in centimeters of injected and uninjected Tcf4 ± mice was measured by Ethovision XT 15.0 program. Only data collected the last 30 min in the chamber was utilized to allow Tcf4 ± mice to equilibrate and begin ambulation within the chamber as previously described [26].

Elevated Zero Maze: As described earlier for Cross Breed Animal Behavioral Assays. Mouse movements on the maze (entries) in open or closed arms are measured by Ethovision XT 15.0 program.

Self-grooming: Mice were placed in a Plexiglas cage with fresh bedding as well as no nest or cardboard material. Self-grooming behavior was recorded automatically by the computer for 10 min following an initial 10 min habituation phase.

Nesting (Activities of Daily Living, ADL): Approximately 1 h before the dark phase, mice were transferred, if housed as a group, to individual testing cages with wood-chip bedding but no environmental enrichment items. Place One Nestlet was placed in each cage after being cut to supply exactly 3.0 g of Nestlet material per cage. The next morning, the nests were assessed a rating scale of 1–5 as described previously [52].

Novel Object Recognition (NOR): Recognition memory for a novel object compared to a familiar object was assessed by the object novelty detection task [55–57]. For this task, a Plexiglas box (26 cm long × 20 cm wide × 16 cm tall) and two objects in duplicate (4–6 cm diameter × 2–6 cm height) were used. Mice were first habituated to the experimental environment by allowing them to freely explore the box without any objects for 20 min per day for 2 consecutive days before testing. During the first session of testing, two copies of Object 1 were placed at each end of the box, and the mouse was allowed to explore the objects for 5 min. The mouse was then removed to an opaque holding container for 5 min, and one object was replaced with Object 2 (novel object) for the mouse to explore during the 5 min test session. More time exploring the novel Object 2 compared to the familiar Object 1 during the test session indicates that the mouse remembered previously exploring Object 1, but equal exploration between the two objects indicates that the mouse has impaired recognition memory. Object exploration is defined as the mouse sniffing or touching the object with its nose, vibrissa, mouth, or forepaws, and time spent near or standing on top of the objects without interacting with the object is not counted as exploration.

Beam walking test: Fine motor coordination and balance was assessed by the beam walking assay in which the mouse had to walk across an elevated horizontal beam (48-cm long, 2.5-cm diameter, 1-m above bedding) to a safe platform. Subjects were placed near one end in bright light, and the far end of the platform was placed in darkness, providing motivation to cross. The performance was quantified by measuring the number of paw slips within a 2-minute cut-off.

Sociability Partition Test: For this study, we followed the Crawley protocol (2014). The social testing apparatus is a rectangular, three-chambered box fabricated from clear Plexiglas. The dividing walls had doorways allowing access into each chamber. An automated tracking system (Ethovision, Noldus is used) provides measures of time spent in each chamber. Each subject was allowed an initial habituation period when they could explore the fully open chamber freely for 10 min. After habituation, the test mouse was enclosed in the center compartment of the social test box. The mouse was placed in one of the side chambers and enclosed in a small Plexiglas cage drilled with holes, allowing for nose contact. An identical empty Plexiglas cage was placed in the opposite side of the chamber. After placement of the mouse and the empty cage, the doors were reopened, and the subject was allowed to explore the social test box for 10 min.

Total Protein Extraction for Cross Bred Animals (Vanderbilt University): The cortex, hippocampus and striatum were microdissected from naïve, 20–25 week old mice. Total protein was prepared as previously described in (Fisher, Gogliotti et al. 2018). Briefly, tissue samples were homogenized using a hand-held motorized mortar and pestle in radio-immunoprecipitation assay buffer (RIPA) containing 10 mM Tris-HCl, 150 mM NaCl, 1 mM ethylenediaminetetraacetic acid (EDTA), 0.1% sodium dodecyl sulfate (SDS), 1% Triton X-100, and 1% deoxycholate (Sigma, St. Louis, MO, USA). After homogenization, samples were centrifuged and the supernatant was collected. Protein concentration was determined using a bicinchoninic acid (BCA) protein assay (Pierce, ThermoFisher, Waltham, MA, USA).

Total Protein Extraction for Injected Animals (University of Chile): Total protein extracts were obtained from the frontal or medial cerebral cortex of PTHS animals. Cortices were dissociated mechanically in cell lysis buffer (TrisHCl 50 mM, NaCl 50 mM, EDTA 1 mM, SDS 0.1%, Triton 1%) with P8340 protease inhibitor (Sigma Aldrich) and disrupted using sonication (Bioruptor Plus, Diagenode) followed by centrifugation at 13,000 rpm for 15 min at 4 °C. Total proteins in the supernatant were quantified using Bradford method.

SDS-PAGE and Western Blotting Protocol for Cross Breed (Vanderbilt University) and In Vitro Cell Analysis (Nationwide Children's): 50 µg of total protein was separated by electrophoresis using a 4–20% SDS polyacrylamide gel and transferred onto a nitrocellulose membrane (Bio-Rad, Hercules, CA, USA). Membranes were blocked in TBS Odyssey blocking buffer (LI-COR, Lincoln, NE, USA) for 1 h at room temperature. Membranes were probed with primary antibodies overnight at 4 °C: rabbit anti-MeCP2 (1:1000, Millipore cat no. 07–013, Burlington, MA, USA) or Anti-TCF-4 antibody - Neuronal Marker (ab185736) and mouse anti-Gapdh (1:1000, ThermoFisher cat. no. MA5-15738, Waltham, MA, USA), followed by the fluorescent secondary antibodies: goat anti-rabbit (800 nm, 1:5000, LI-COR, Lincoln, NE, USA) and goat anti-mouse (680 nm, 1:10,000, LI-COR, Lincoln, NE, USA). Fluorescence was detected using the Odyssey Infrared Imager (LI-COR, Lincoln, NE, USA) at the Vanderbilt University Medical Center Molecular Cell Biology Resource (MCBR) Core then quantified using the Image Studio Lite software (LI-COR, Lincoln, NE, USA). Values were normalized to Gapdh and compared relative to wild-type controls.

SDS-PAGE and Western Blotting Protocol for Injected Animals (University of Chile): Samples were heated at 95 °C for 5 min for denaturation and resolved by SDS-PAGE in a 10% (w/v) polyacrylamide gel and transferred to PVDF membranes (0.45 µm, Immobilon-P, Merck Millipore, Germany); membranes were blocked with 5% milk and incubated overnight at 4 °C with rabbit anti-MeCP2 (D4F3, Cell Signalling, 1/800) or mouse anti-actin (sc-69879, Santa Cruz, 1/2000) antibodies. Membranes were then incubated with secondary antibodies, including HRP-conjugated anti-mouse or anti-rabbit (1/5000, R&D systems). Immunoreactive proteins were detected using enhanced chemiluminescence reagents according to the manufacturer's instructions (SuperSignal West Pico Plus Chemiluminescent substrate, Thermo scientific).

Total RNA Extraction: The hippocampus and striatum were microdissected from naïve 20–25 week old mice. Total RNA was prepared from tissue samples using TRIzol Reagent (ThermoFisher, Waltham, MA, USA) and isolated using an RNeasy Mini Kit (Qiagen, Hilden, Germany) in accordance with manufacturer's instructions. Total RNA was DNase-treated with RNase-Free DNase Set (Qiagen, Hilden, Germany). Using one set of RNA samples, cDNA from 2 µg of total RNA was synthesized using SuperScript™ VILO™ cDNA Synthesis Kit (ThermoFisher cat no. 11754050, Waltham, MA, USA) for qRT-PCR analysis.

Quantitative Real-Time PCR (qRT-PCR): RT-qPCR (CFX96, Bio-Rad Hercules, CA, USA, equipment located at the Vanderbilt University Medical Center MCBR core) on 50ng/9 µL cDNA was run in duplicate using PowerUp™ SYBR™ Green Master Mix (ThermoFisher cat no. A25742, Waltham, MA, USA) with primers for target genes (Supplementary Table 1). Ct values for each sample were normalized to Gapdh expression and analyzed using the delta–delta Ct method as described in

Ref. [28]. Values exceeding two times the standard deviation were classified as outliers. Each value was compared to the average delta-Ct value acquired for wild-type controls and calculated as percent-relative to the average control delta-Ct.

Statistical Analyses: Statistics were carried out using Prism 8.0 (GraphPad) and Excel (Microsoft). All data shown represent Mean \pm SEM. Statistical significance between genotypes was determined using mixed-effects analysis, or nonparametric statistical tests (Mann-Whitney U test, 1-way or 2-way ANOVA with Sidak's or Tukey's post-hoc test). Sample size and statistical test are specified in each figure legend or on the graph above the error bars.

Results

TCF4 patient iNPCs have reduced MeCP2 protein levels affecting astrocyte differentiation and function

We utilized three different patient skin-derived fibroblast cell lines from PTHS patients harboring different mutations (c.1486+5G>T, c.520C>T, del [18] (q21.2q21.32), [Supplementary Fig. 1a](#)). The fibroblasts were directly reprogrammed to iNPCs according to previously established methods [10–15]. We first quantified the levels of TCF4 protein (approximately 70 kDa, corresponding to isoforms B,D,E,F,M,NO, Q) via Western blot. There was no significant change in the levels of TCF4 in patient fibroblasts or NPCs relative to healthy controls ([Fig. 1a and b](#)). Next, we evaluated MeCP2 levels in each cell line. While no significant changes in MeCP2 protein levels were found in any of the patient fibroblast cell lines ([Fig. 1c](#)), all PTHS iNPCs displayed a significant reduction of MeCP2 compared to healthy controls ([Fig. 1d](#)). Astrocytes have recently been described to play an important role in Rett Syndrome [16–18]. To evaluate disease mechanisms in astrocytes, iNPCs were further differentiated into induced Astrocytes (iAs) as previously described [10–12]. Given that astrocytes are primarily glycolytic, we evaluated cellular glycolysis and oxygen consumption in patient iAs through the extracellular acidification rate (ECAR). We found patient cell line-specific alterations in cellular glycolysis as well as significantly reduced basal and ATP-linked respiration in all three patient iAs ([Fig. 1e](#)). Since astrocytes have a major role in support of neurons, we evaluated the non-cell autonomous effect of PTHS iAs on neuronal morphology and survival in established co-culture assays as previously described [10–13]. Co-culture of patient iAs with healthy mouse neurons demonstrated that all three patient cell lines significantly impacted neuronal morphology and/or survival ([Fig. 1f and g](#)). Interestingly, TCF4-3 also displayed severe defects in differentiation from iNPCs to astrocytes, as indicated by continued expression of high nestin levels and strongly reduced levels of the astrocyte marker, glial fibrillary acidic protein, GFAP compared to healthy controls and the other two PTHS cell lines ([Supplementary Fig. 1b](#)) [10–15].

Genetically increasing MeCP2 expression does not affect Tcf4 mRNA levels

To determine whether elevating MeCP2 levels affects PTHS phenotypes *in vivo*, we crossed *Tcf4*^{+/-} mice with a mouse expressing an autosomal *MECP2* transgene, *MECP2*^{Tg1/0} ([Fig. 2a](#), [19]) at Vanderbilt University. The *MECP2*^{Tg1/0} mouse expresses ~2x MeCP2 levels relative to WT mice and is commonly used as a model of a related neurodevelopmental disorder termed *MECP2* Duplication Syndrome (MDS). The *MECP2*^{Tg1} allele has also previously been used to rescue phenotypes in knock-in and truncating mouse models of RTT [20–25]. We bred *MECP2*^{Tg1/0} animals with *Tcf4*^{+/-} mice to generate *MECP2*^{Tg1/0}; *Tcf4*^{+/-} transgenic mice that are haploinsufficient for *Tcf4*, have a wild type murine *Mecp2* locus, and a third *MECP2* allele from the transgene ([Fig. 2a](#)), which cannot be distinguished from each other. To confirm that MeCP2 was appropriately increased, we harvested cortex, hippocampus,

and striatum and conducted quantitative PCR and Western blot analysis. As expected, *MECP2*^{Tg1/0} animals had significantly higher levels of MeCP2 mRNA and protein relative to wildtype and *Tcf4*^{+/-} controls in the cortex, hippocampus, and striatum. No difference in MeCP2 levels was seen in *Tcf4*^{+/-} animals compared to wildtype controls ([Fig. 2b–d](#)). *MECP2*^{Tg1/0}; *Tcf4*^{+/-} offspring retained the elevated levels of MeCP2 with no impact on *Tcf4* mRNA expression ([Fig. 2e](#)), regardless of the brain region. Notably, *MECP2*^{Tg1/0}; *Tcf4*^{+/-} mice resemble *MECP2*^{Tg1/0} mice in terms of the level of MeCP2 protein expression ([Fig. 2c and d](#)). However, analysis of *Tcf4*^{+/-} transgenic mice at an earlier age (p60), at an independent lab at the University of Chile, revealed reduced MeCP2 expression levels in frontal and medial cortex ([Supplementary Fig. 2](#)), suggesting that subregions of the cortex may be unique in their relationship between *Tcf4* heterozygosity and *Mecp2* expression. To evaluate the relationship between *Tcf4* and MeCP2, we next quantified *Tcf4* mRNA levels ([Fig. 2e](#)). These studies revealed significant reductions in *Tcf4* mRNA in both *Tcf4*^{+/-} and *MECP2*^{Tg1/0}; *Tcf4*^{+/-} double transgenic mice that were significantly decreased compared to wild-type controls. These data indicate that increasing MeCP2 dosage does not impact on *Tcf4* mRNA levels in healthy control or *Tcf4*^{+/-} mice.

Abnormal phenotypes in Tcf4+/- mice are reversed with increased MeCP2 dosage

To determine whether increased MeCP2 expression normalized disease phenotypes *in vivo*, we performed a battery of behavioral tests, focusing on previously identified abnormal behavioral characteristics of various PTHS model mice [26]. Consistent with previous reports, *Tcf4*^{+/-} mice showed significant hyperlocomotor activity in an open field while *MECP2*^{Tg1/0} mice showed no difference relative to control animals ([Fig. 3a and b](#)). In support of our hypothesis, hyperlocomotor activity was reduced to WT levels in *MECP2*^{Tg1/0}; *Tcf4*^{+/-} test mice, with similar distance travelled compared to littermate controls. Additionally, *Tcf4*^{+/-} mice displayed a significant increase in vertical or rearing activity in the open field arena and increased expression of MeCP2 also attenuated this behavior ([Fig. 3c](#)). Given that rearing has been linked to anxiety-related behavior [27], we performed an additional assay to measure anxiety using an elevated zero maze apparatus. In this test, *Tcf4*^{+/-} animals spent more time in the open, fully lighted regions of the maze, displaying significantly diminished anxiety ([Fig. 3d](#)). This phenotype was also corrected in *MECP2*^{Tg1/0}; *Tcf4*^{+/-} mice, correlating with reduced time spent in the open regions [28–32].

Elevation in MeCP2 levels in PTHS patient cell line restores defective iNPC to astrocyte differentiation and astrocyte-mediated neuronal support

Given the promising efficacy of increasing MeCP2 levels via genetic cross in *Tcf4*^{+/-} mice, we next tested an AAV9-based gene therapy approach in our PTHS patient cell lines. The iNPCs containing the deletion mutation that showed a severe defect in differentiation in our previous assays were transduced with AAV9.P546.MeCP2 and the differentiation potential into iAs was re-evaluated. Increased MeCP2 mRNA and protein levels following transduction were confirmed in iAs 5 days following transduction ([Supplementary Fig. 3](#)). Remarkably, immunofluorescent staining indicated that transduction of the iNPCs prior to iA differentiation led to improved differentiation as demonstrated by a decrease in nestin signal and an increase in GFAP signal ([Fig. 4a and b](#)). Moreover, in co-culture, AAV9.P546.MeCP2-transduced iAs from this patient were now better able to support neuronal survival, as well as improve neuronal morphology as indicated by an increased number of neurites and skeleton length ([Fig. 4c and d](#)). Combined, these data suggest that increasing MeCP2 levels in defective PTHS iNPCs results in improved iA differentiation and improved support of co-cultured neurons.

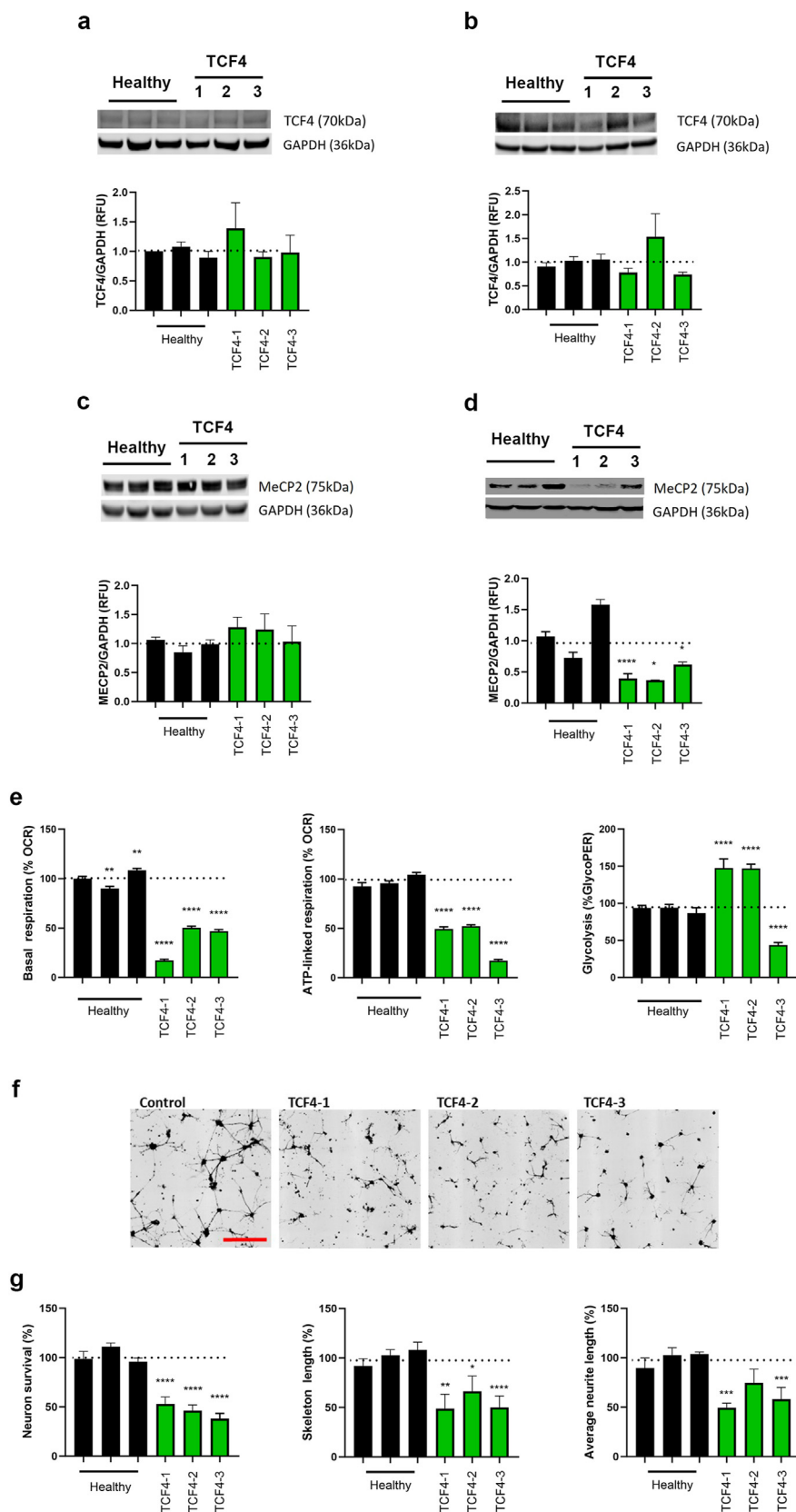


Fig. 1. Patient fibroblast-derived NPCs have reduced MeCP2 levels and exhibit reduced ability to differentiate into astrocytes.

Fibroblast (A and C) and NPC (B and C) lysates were analyzed by Western blot and levels of TCF4 (A and B) and MeCP2 (C and D) were quantified. NPCs were subsequently differentiated into astrocytes and their metabolic state, in addition to impact on neurons, was evaluated. E) Extracellular flux analysis was used to quantify oxygen consumption rate (OCR) and extracellular acidification rate (ECAR) to determine mitochondrial basal respiration, ATP-linked respiration and glycolytic protein efflux rate (glycoPER). Mitochondrial-based respiration was down-regulated in TCF4 mutant astrocytes and a mutation-specific effect on glycoPER was identified (as measured by lactate mediated acidification). F) Representative images of neurons co-cultured with differentiated astrocytes (scale bar: 200 μ M). G) Quantification of survival and neuronal morphology. Neurons cultured on TCF4 patient-induced astrocytes have reduced survival and shorter neurite and skeletal length. Dotted line represents average control values. Data have been generated from at least 3 independent experiments. Statistical analysis was performed using One-way ANOVA with Dunnett post-hoc analysis comparing the mean of each data set to the combined average of the controls (dotted line). * $p < 0.05$, ** $p < 0.01$, *** $p < 0.001$, **** $p < 0.0001$.

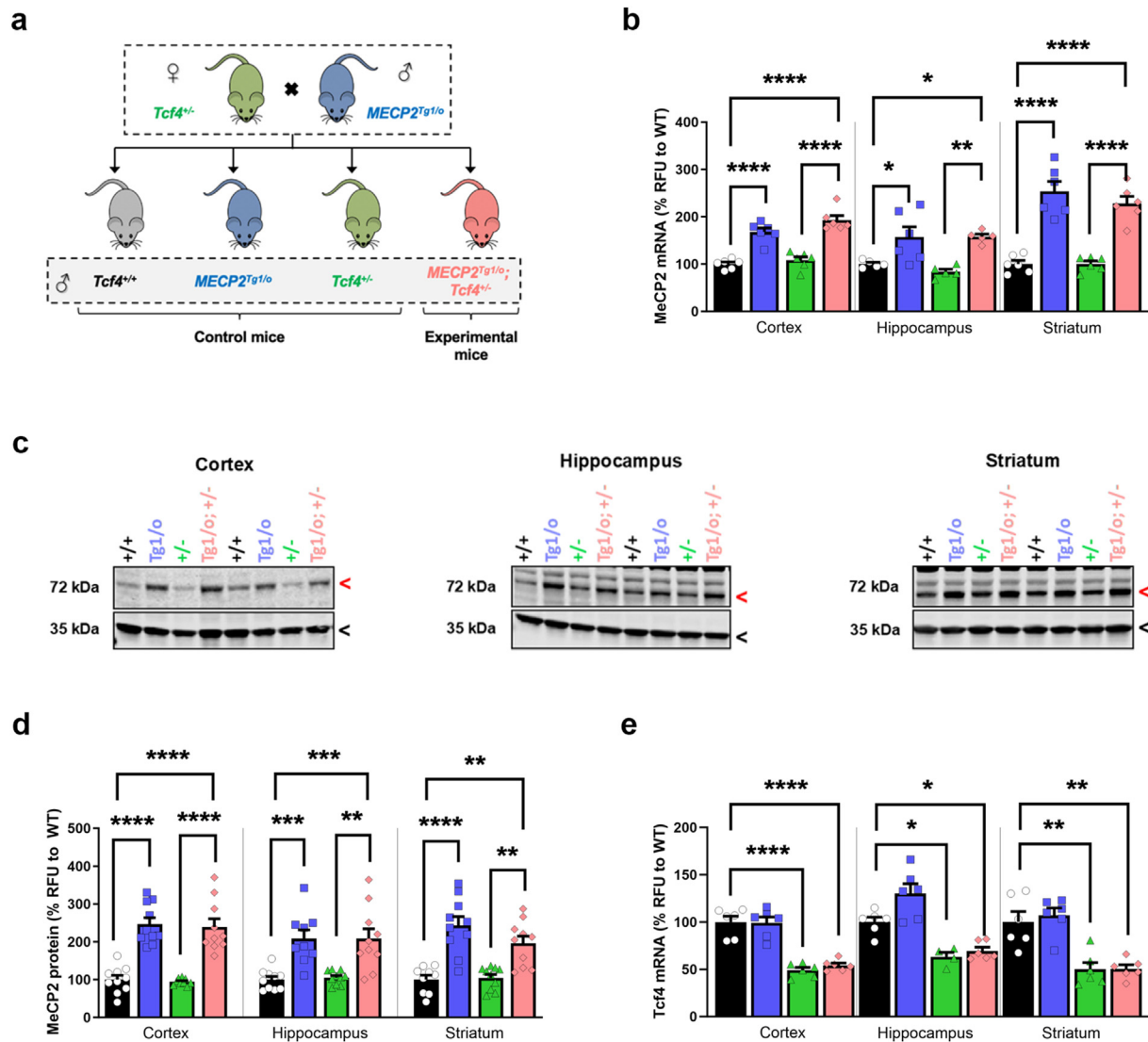


Fig. 2. Increased MeCP2 dosage does not affect Tcf4 expression in mice.

(A) Breeding scheme to genetically introduce the *MECP2* transgene (*MECP2^{Tg1/o}*) into *Tcf4^{+/-}* animals. MeCP2 mRNA (B) and protein levels (C-D) were quantified in the cortex, hippocampus and striatum of wildtype (*Tcf4^{+/+}*, black), *MECP2^{Tg1/o}* (blue), *Tcf4^{+/-}* (green), and *MECP2^{Tg1/o}; Tcf4^{+/-}* (pink) P120 mice. (B) qPCR with values normalized to corresponding wild type controls. MeCP2 mRNA expression was significantly increased in the presence of the Tg1 transgene and was not affected by Tcf4 heterozygosity. (C) Representative images of fluorescent Western blot for MeCP2/Mecp2 (72 kDa, red arrow) and Gapdh (35 kDa, black arrow). (D) MeCP2 protein (72 kDa band) levels were normalized to Gapdh (35 kDa band) and then normalized against the corresponding wildtype controls. MeCP2 protein levels were elevated in *MECP2^{Tg1/o}* and *MECP2^{Tg1/o}; Tcf4^{+/-}* mice. (E) Tcf4 mRNA expression is decreased in the brains of *Tcf4^{+/-}* and *MECP2^{Tg1/o}; Tcf4^{+/-}* mice, but is unaffected by the Tg1 transgene. mRNA: n = 5–6 mice per genotype. Protein: n = 9–10 mice per genotype. 1-way ANOVA with Tukey's post-hoc test within each brain region. *p < 0.05, **p < 0.01, ***p < 0.001, ****p < 0.0001. Open circle/black bars = *Tcf4^{+/+}*, blue squares/bars = *MECP2^{Tg1/o}*, green triangles/bars = *Tcf4^{+/-}*, pink diamonds/bars = *MECP2^{Tg1/o}; Tcf4^{+/-}*.

AAV9.P546.MeCP2 treatment effectively ameliorates disease phenotype in *Tcf4^{+/-}* mice

Our *in vitro* and transgenic rescue experiments established proof-of-concept that increasing MeCP2 dosage from conception can rescue PTHS phenotypes. We next tested the therapeutic potential of post-natal AAV9 based delivery of MeCP2 in *Tcf4^{+/-}* mice at the University of Chile, a third independent laboratory. Postnatal day 1 (PND1) pups were injected via intracerebroventricular injection (ICV) with 1.5×10^{10} vg scAAV9.P546.MeCP2, a dose previously established to be efficacious for treatment of RTT syndrome in *Mecp2^{0/y}* knockout mice as performed by the Meyer lab [32]. The injection route and dose allows widespread targeting of the brain and spinal cord as demonstrated in previous publications [28–32]. Therapeutic impact was evaluated using open-field, self-grooming, social interaction test, nesting, novel item recognition,

and beam walk at 60 days. In these experiments, *Tcf4^{+/-}* mice again showed hyperactivity, elevated rearing, and spent more time in the open areas of the plus maze. Importantly, *Tcf4^{+/-}* mice injected with scAAV9.P546.MeCP2 showed significant rescue in all three of these phenotypes relative to uninjected control mice, with normalized activity (Fig. 5a), decreased rearing (Fig. 5b), and a reduction in time spent in the open arms (Fig. 5c).

We next evaluated stereotypic behaviors by quantifying self-grooming frequency. In this test, *Tcf4^{+/-}* mice exhibited significantly more grooming behaviors than *Tcf4^{+/+}* animals, and injection with scAAV9.P546.MeCP2 resulted in a significant reduction in grooming habits relative to uninjected *Tcf4^{+/-}* mice (Fig. 5d). To assess sociability, we employed a social interaction test that quantifies the amount of time spent in a chamber with a novel mouse following 10 days of isolation. In this experiment, *Tcf4^{+/+}* mice spent significantly more time in the

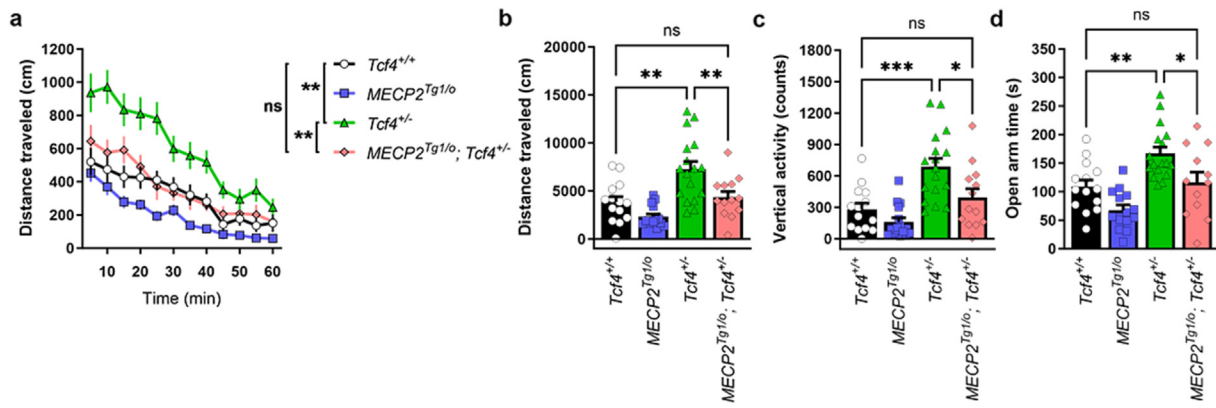


Fig. 3. Increasing MeCP2 levels reverses abnormal phenotypes in *Tcf4*^{+/-} mice.

(A–B) *Tcf4*^{+/-} mice (20–26 weeks of age) exhibit hyperlocomotive activity in an open field chamber, (C) enhanced vertical activity in an open field chamber, and (D) increased time spent in the open arms of an elevated zero maze (green versus black bars). All of these abnormal responses in *Tcf4*^{+/-} compared animals are normalized to *Tcf4*^{+/+} levels in the presence of the MeCP2 transgene. *n* = 8–16 mice per genotype. Statistical analysis was performed using 1-way ANOVA with Tukey's post-hoc test. **p* < 0.05, ***p* < 0.01, ****p* < 0.001, *****p* < 0.0001, ns (not significant) for panels B, C, and D and 2-way ANOVA was used in time course locomotion data (A). Open circle/black bars = *Tcf4*^{+/+}, blue squares/bars = *MECP2*^{Tg1/0}, green triangles/bars = *Tcf4*^{+/-}, pink diamonds/bars = *MECP2*^{Tg1/0}; *Tcf4*^{+/-}.

chamber holding the novel mouse than that with the empty cage, while *Tcf4*^{+/-} mice spent significantly more time in the empty cage, suggesting a preference for social isolation. In contrast, scAAV9.P546.MeCP2-treated *Tcf4*^{+/-} mice spent significantly more time in the chamber with the novel mouse to a degree that matched wild-type controls (Fig. 5e). Next, we assessed nesting as a measure of daily living activities to evaluate the performance of species-related tasks [33]. Wildtype *Tcf4*^{+/+} animals made nests achieving scores between 4 and 5 while *Tcf4*^{+/-} mice scored a median score of 2. In contrast to *Tcf4*^{+/-} mice, treated *Tcf4*^{+/-} scored 4.5 in nesting, which was comparable to wildtype levels (Fig. 5f).

As a measure of spatial learning, we tested mice in the novel object recognition task. Wildtype animals spend more time investigating novel objects than they do with objects to which they have been previously exposed. In contrast, *Tcf4*^{+/-} failed to differentiate between the novel and familiar mouse indicating learning and memory deficits (Fig. 5g). Importantly, the learning and memory deficit of treated mice improved time spent recognizing novel objects as these animals spent more time investigating novel objects when compared to familiar objects. Finally, we evaluated motor coordination in *Tcf4*^{+/-} mice using the beam walk assay. Notably, *Tcf4*^{+/-} mice had more slips than wild-type littermates, which were not corrected by treatment with the viral construct (Fig. 5h). Combined, these data demonstrate that scAAV9.P546.MeCP2 effectively reduces anxiety, restores species-related tasks, learning and memory in treated *Tcf4*^{+/-} mice.

scAAV9.P546.MeCP2 treatment improves neuronal morphology in *Tcf4*^{+/-} animals

To determine whether phenotypic improvement correlated with rescue of neuronal morphology as observed *in vitro*, we performed an imaging analysis of CA1 pyramidal neurons 120 days post treatment. Fig. 6a–c depicts representative images of CA1 pyramidal cells obtained from the virally-treated and untreated *Tcf4*^{+/-} mice compared to WT controls. When compared to WT, both untreated and AAV9.P546.MeCP2-treated *Tcf4*^{+/-} mice displayed significant shorter dendritic length (upper panel, A to C, Scale bar: 50 μm) as well as reduced number and density of dendritic spines of CA1 pyramidal cells (boxes in the lower panel, A' to C'; Scale bar: 5 μm). However, when comparing the untreated *Tcf4*^{+/-} mice to the AAV9.P546.MeCP2 treated animals, we found that treated *Tcf4*^{+/-} mice had significantly longer dendritic length compared to untreated animals (Fig. 6d). This increase was true for both apical and basal dendrites (Fig. 6e and f). A similar pattern was also observed in spine counts (Fig. 6g–i) and overall spine density (Fig. 6j–l), where both treated and untreated exhibited decreased counts and density

relative to controls (Fig. 6g and j), but treated *Tcf4*^{+/-} mice were significantly improved relative to untreated mice in both number and density of basal and apical dendritic spines (Fig. 6h,i,k,l). Combined, these data demonstrate that elevating MeCP2 levels postnatally by treatment with AAV9.P546.MeCP2 significantly improves pyramidal cell morphology in *Tcf4*^{+/-} mice.

Discussion

The neurodevelopmental disorder PTHS displays many similarities to RTT, including intellectual disability, global developmental delay, breathing abnormalities, stereotypic hand movements, seizures, and sleep disturbances, which could indicate potential shared disease pathways. Patients who are diagnosed with atypical RTT based on symptoms but are not found to carry mutations in *MECP2* are often found to have mutations in *CDKL5*, *FOXG1*, *TCF4* or other genes [34, 35]. The overlap in symptoms points to similarly disrupted pathogenic mechanisms and, therefore, the possibility to explore whether the same treatment could benefit for multiple disorders. Here, we tested the hypothesis that MeCP2 might be involved in pathology of PTHS using reprogrammed patient cells as well as mouse models. Testing was performed in three different independent laboratories to ensure maximum rigor. We quantified reduced MeCP2 levels in iNPCs of PTHS patients harboring different types of mutations compared to healthy controls. A reduction of MeCP2 levels was then also confirmed in the *Tcf4*^{+/-} mouse model at 60 days of age in one of the *Tcf4*^{+/-} colonies used in this study. In contrast, no difference in TCF4 levels were observed in the genetic crossing study that was conducted in an independent mouse colony. These findings may be explained by the molecular pathology observed in RTT patients. It has previously been shown that RTT patients have, most distinctively, altered MeCP2 expression in the frontal cerebrum compared with hippocampus, amygdala and cerebellum [36]. This was accompanied with evidence pointing to regional regulation of MeCP2 transcripts, although MeCP2 homeostasis regulation is still not understood. In consequence, whole brain or cortex lysate might obscure regional changes. Furthermore, regional changes can be dynamic as shown by age dependent effects from 3 to 9 months of MeCP2 heterozygosis on X chromosome inactivation [37]. Thus, it is currently unclear whether MeCP2 levels are specifically lower in younger *Tcf4*^{+/-} animals and normalize at later ages or if the molecular defects are limited within a select region of the cortex which was not captured in the sample lysates. In addition, variances in the colonies or experimental methods may also explain the discrepancy in MeCP2 levels between the two studies. Further studies

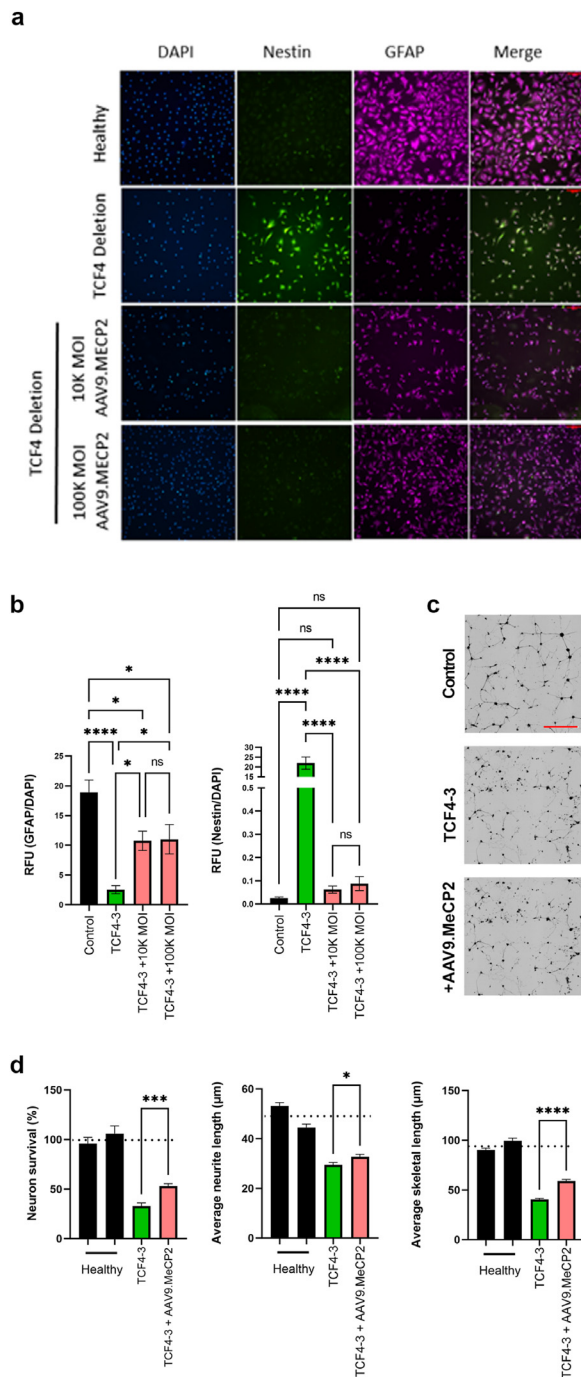


Fig. 4. Treatment of patient fibroblast-derived NPCs with AAV9.MECP2 restores differentiation potential into astrocytes that are supportive of neuron morphology and survival.

NPCs were transduced with AAV9.MECP2 and subsequently differentiated into astrocytes. (A) Cells were stained with the NPC marker, nestin, and an astrocyte marker, GFAP. (B) Quantification of GFAP and nestin staining intensity following differentiation. Transduction with AAV9.MECP2 improved differentiation potential as indicated by reduced nestin and increased GFAP staining (scale bar: 100 µm). Astrocytes were seeded in co-culture with GFP⁺ neurons (black) and imaged 3 days later. (C) Representative images of neurons co-cultured with differentiated astrocytes. (D) Quantification of survival and neuronal morphology (scale bar: 200 µm). AAV9.MECP2 significantly improved survival and neuronal morphology in the TCF4 deletion line (TCF4-3). Dotted line represents average control values. Data were generated from at least 3 independent experiments. Statistical analysis was performed using Student's T-test comparing the mean of untreated vs treated TCF4 cell lines. *p < 0.05, **p < 0.01, ***p < 0.001, ****p < 0.0001.

requiring multiple time points and more detailed region and cell type-specific analyses might be necessary to understand MeCP2 dynamics in *Tcf4*^{+/-} in detail.

Despite these discrepancies in MeCP2 measurements, both the independently conducted genetic rescue study and the therapeutic gene replacement study indicate a clear benefit from increased MeCP2 expression. Crossing MeCP2 overexpressing mice with *Tcf4*^{+/-} mice significantly improved behavioral abnormalities, providing significant genetic evidence of the importance of MeCP2 in PTHS pathology as well as a lack of development of MDS-like behavioral effects. Treatment of PTHS patient cell lines with the AAV gene replacement therapeutic vector scAAV9.P546.MeCP2 improved cellular differentiation and function *in vitro*. The effect of the viral construct was then further confirmed in *Tcf4*^{+/-} mice in an independent lab, where improved neuronal morphological defects and significantly ameliorated cognitive, behavior (anxiety, learning and memory) and motor function were quantified. It is important to note that the factors that contribute to performance in behavioral assays are often interconnected, and the reasons that underlie the observed improvements can be multifactorial. In the case of *Tcf4*^{+/-} mice, the hyperactivity phenotype could be a confounding factor for the assessment of sustained attention, given that the general activity of the mutant mice may interfere with task engagement. For example, novel object recognition is typically conducted as a short-term memory task and relies on rodents' natural tendency to investigate novelty. Thus, the time spent with a novel object could be reduced not because an animal recognizes the object, but because the animal is hyperactive in the first place. Nevertheless, the simultaneous improvement of several independent behavioral phenotypes using both genetic and therapeutic gene replacement therapy approaches to raise MeCP2 levels supports the importance of MeCP2 in PTHS pathology and the potential of common therapeutic targets between RTT and PTHS.

The exact mechanism by which an increase in MeCP2 levels provides therapeutic benefit in PTHS is currently unknown and further studies will be needed to unravel the pathways involved. Our promising results may point to three possible mechanisms by which elevating MeCP2 is therapeutic. The first mechanism maybe be a consequence of selectively increasing MeCP2 levels in cell types critical for disease pathology. Our data from human patient cell lines demonstrated significantly reduced levels of MeCP2 in iNPCs but not in the fibroblasts. Hence, MeCP2 levels might only be affected in certain cell types of PTHS patients. Importantly, elevating MeCP2 levels in the iNPCs resulted in enhanced differentiation and function of the astrocytes. While this was not a full rescue, AAV9 transductions *in vitro* are notoriously difficult and technical challenges, such as a short period of MeCP2 elevation, could explain the partial response. Nevertheless, these data suggest that at least some of *in vivo* rescue might be linked to normalizing deficient MeCP2 expression in progenitor cells. The importance of neuronal progenitor cell dysfunction in PTHS and RTT has recently been described by several other groups who have also observed deficits in progenitor proliferation, differentiation, or function ([38–44] reviewed in Ref. [45]). The data reported here is novel and distinct from these previous studies as we used three types of patient mutations (deletion, missense and frameshift mutations) and report for the first time that these cells display a significant down-regulation of MeCP2. The finding that an increase in MeCP2 levels ameliorates cellular phenotypes has not been explored to date. The second possibility is that shared downstream pathways of MeCP2 and TCF4 may present an opportunity for MeCP2-mediated signaling to counteract the loss of TCF4-mediated signaling. In doing so, key pathways contributing to developmental and behavioral phenotypes may be restored sufficiently to show a therapeutic effect. It will be interesting in future studies to evaluate changes in genes of interest in neuronal progenitor cells in the context of manipulating MeCP2 levels, which could help identify common downstream pathways. Finally, we cannot eliminate the possibility that antiparallel phenotypes in *Tcf4*^{+/-} and *MeCP2*^{Tg1/0} mice are normalized due to their opposite effects on behavior. While this may explain the some of the promising results in the transgenic crosses

and the therapeutic treatment of the mice, it is less likely to explain the observed beneficial effect observed in the patient iNPCs.

On the surface, the reversal effect of increased MeCP2 dosage in *Tcf4*^{+/-} mice could be viewed as surprising, as previous studies have established that MDS-like phenotypes are observed with overexpression of MeCP2 [23,24]. However, we and several other groups have developed MeCP2 gene therapy viral vectors that allow expression of MeCP2 at levels that are well tolerated even in wildtype mice [32,46,47] and nonhuman primates (NHPs) [32]. We have studied the safety profile of this same viral vector construct extensively in previous published work [32]. The therapeutic dose selected in this study was tested in wildtype mice, with normal levels of MeCP2, and was shown to have no adverse effects on survival or behavior. Safety of this viral vector construct was further confirmed in five nonhuman primates (NHP) using clinically relevant dosages. Weight, serum chemistry and hematology was routinely monitored for up to 18 months post treatment at which time the animals were sacrificed for an extensive pathological evaluation of

relevant tissue. Findings from this study showed normal behavior, body weight and bloodwork and histopathological evaluation confirmed that the treatment was safe and well tolerated [32]. [48,49] Moreover, several groups are currently advancing MeCP2 gene replacement therapies to the clinic (NCT05898620, NCT05606614). If these treatments prove to be safe and efficacious, the therapeutic approach may be adapted to PTHS patients. In contrast, development of a TCF4-specific gene therapy is more complex due to the large number of isoforms that have been reported for the gene, and it is unclear if replacing only one isoform would be sufficient to provide substantial clinical benefit. Thus, further research evaluating the mechanisms behind this novel therapeutic approach and its feasibility should be conducted.

For small rodents, nests are important in heat conservation as well as reproduction, shelter, and innate behavior. In 2005, it was proposed that the hippocampus is also vital for the performance of species-typical tasks such as nesting [33]. Follow-up studies suggest that the impact of dorsal and ventral regions of the brain do not directly impact nesting but are additive in phenotype severity [50–53]. Specifically, Deacon (2006) published that mice with hippocampal lesions scored between 0 and 3, with only the completely lesioned mice showing inhibition of nesting. Interestingly, *Tcf4*^{+/-} mice scored a median score of 2, indicating that the nestle material was not fully taken apart to generate a nest. Thus, these data support previous observations that *TCF4* mutations result in hippocampal deficits [26] but not substantial hippocampal damage. This suggests that neurological impairments in *Tcf4*^{+/-} animals may be reversible with a treatment that improves hippocampal function. Importantly, treatment of *Tcf4*^{+/-} animals with scAAV9.P546.MeCP2 increased nesting scores to levels comparable to healthy controls. These data suggest that elevating MeCP2 levels is sufficient to restore hippocampal function and, more importantly, that hippocampal dysfunction related to loss of TCF4 activity might be treatable at least when addressed early after birth. Additional experiments will be required to confirm a benefit at later treatment time points in follow up studies.

Further evidence of the importance of hippocampal function in PTHS comes from recent studies of neuronal progenitor cells which show defects in adult neurogenesis in the hippocampus [38–40]. Our data shows that *Tcf4*^{+/-} animals have reduced dendrite length, spine counts and

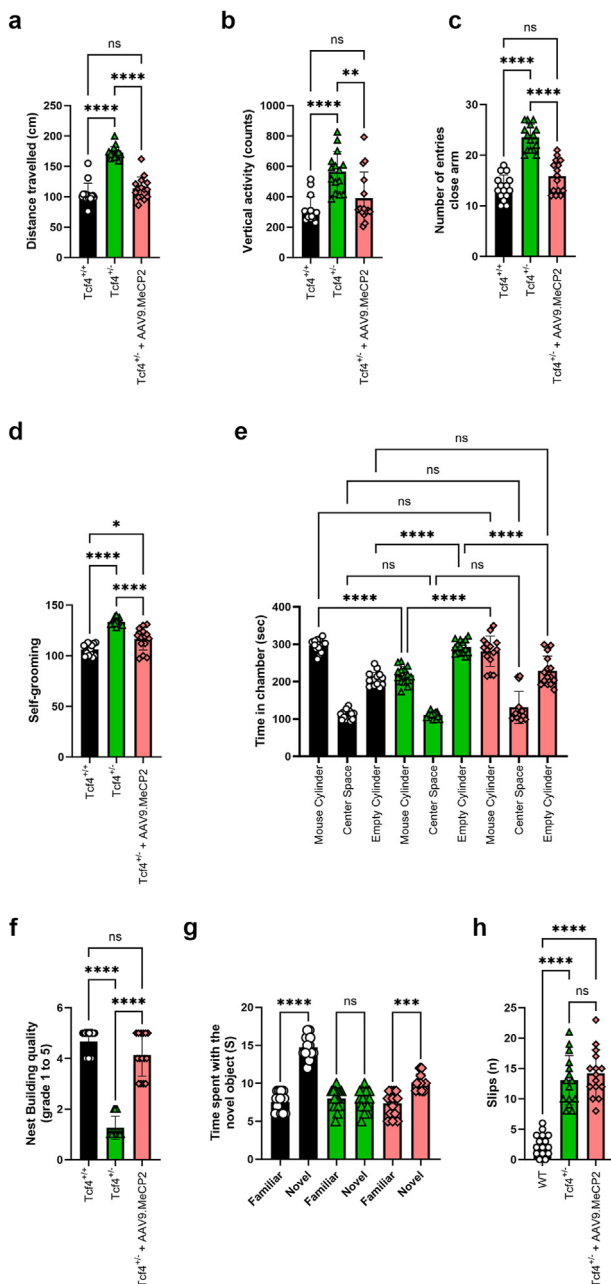
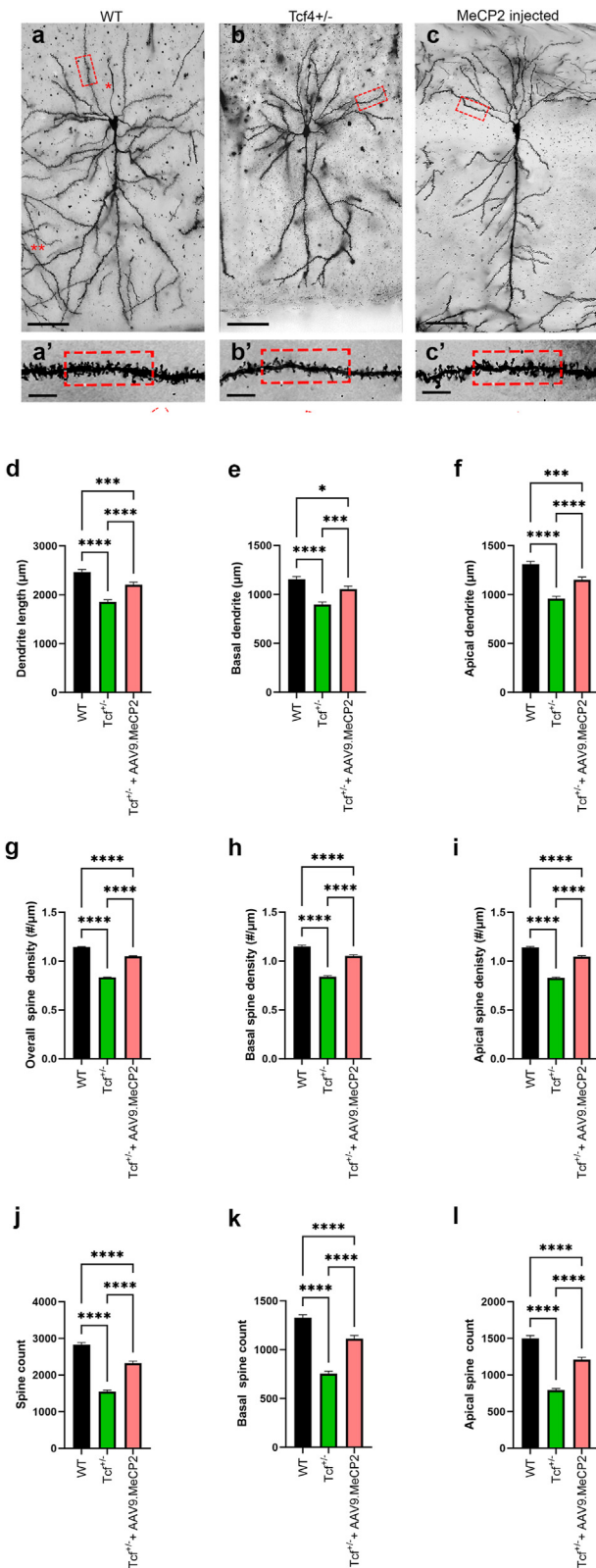


Fig. 5. AAV9 delivery of MeCP2 reverses disease phenotypes in *Tcf4*^{+/-} mice.

Tcf4^{+/-} pups were injected at p1 with scAAV9.P546.MeCP2. Fifteen mice per treatment group were aged to p60 prior to motor and behavioral analysis. (A) After 30 min, *Tcf4*^{+/-} mice showed hyperactivity in the open field and treatment with scAAV9.P546.MeCP2 significantly normalized the distance travelled compared to *Tcf4*^{+/+} littermates. Anxiety levels were quantified by number of rearing events in the open field (B) and the number of times a mouse entered the closed arm of the elevated plus maze within a 5 min period (C). Treatment with scAAV9.P546.MeCP2 significantly reduced rearing and time spent in the closed arm in *Tcf4*^{+/-} treated mice. (D) Time spent self-grooming was significantly elevated in *Tcf4*^{+/-} mice and rescued by scAAV9.P546.MeCP2 injection when compared to untreated controls. (E) Three chamber social interaction. Relative to littermate controls, *Tcf4*^{+/-} mice spend significantly more time with the empty cylinder, and this deficit is partially rescued by the scAAV9.P546.MeCP2 construct. (F) Nesting activities were quantified by transferring mice into a test cage containing 3 g of a Nestlet and the next morning nests were scored on a scale of 1–5 (5 being normal) as described in Materials and Methods. scAAV9.P546.MeCP2-injection significantly improved nesting capabilities when compared to uninjected controls. (G) Novel Object Recognition. *Tcf4*^{+/-} mice do not distinguish between familiar and novel objects, and the recognition/preference for the novel object was restored by scAAV9.P546.MeCP2-injection. (H) The number of total slips of *Tcf4*^{+/-} and WT littermates was evaluated using a Beam Walk test. The number of foot faults was counted in treated and untreated animals and compared to WT (*Tcf4*^{+/+}) mice. scAAV9.P546.MeCP2 treatment significantly reduced the number of foot falls when compared to untreated animals. Statistical analysis was performed using one way ANOVA followed by Sidak's (A, B, C, E, H), Dunnett's (D) or Dunn's (G, F) post hoc test. *p < 0.05, **p < 0.01, ***p < 0.001, ****p < 0.0001.

(caption on next column)



(caption on next column)

overall spine density. Treatment with the MeCP2-vector caused a significant improvement in the morphological characteristics of CA1 pyramidal cells in *Tcf4*^{+/-} mice. These MeCP2-induced increases in spine density were attributed to changes in basal and apical dendrites of CA1 pyramidal cells. Given that CA1 pyramidal neurons are key cell types in the hippocampal memory system, deficits in the morphology of these cell types suggest aberrancies in learning and memory pathways that may be reversed by increasing MeCP2 levels.

Taken together, our study involving three independent laboratories, patient cell lines and two *Tcf4*^{+/-} mouse colonies indicate an important role of MeCP2, the protein whose loss causes RTT, in PTHS pathology. Our study highlights potential mechanistic overlap between these neurodevelopmental disorders that warrant exploring common therapeutic strategies moving forward.

Author Contributions

At Vanderbilt: S.A.D.V, R.G.G., and C.M.N. designed the experiments. S.A.D.V., A.B., K.W., Y.M., and H.R. performed the experiments and subsequent analyses. S.A.D.V.

At University of Chile: R.D. performed all the behaviour experiments. A.S.A. and F.D.E. performed the P0 transcranial injections and molecular biology experiments. P.C. planned the behavior experiments at P60.

At Nationwide Children's: A.D.S., K.R., and J.Z. performed the experiments and did the data analysis with C.N.D. input and supervision. S.P. designed experiments. K.C.M. supervised experiments, reviewed data, and supported analysis.

C.N.D., K.C.M., K.R., R.G.G. and C.M.N. wrote and edited the manuscript with input from all authors.

Declaration of competing interest

The authors declare the following financial interests/personal relationships which may be considered as potential competing interests: Kathrin C Meyer, Patricia Cogram, Colleen M. Niswender reports financial support was provided by Pitt Hopkins Research Foundation. Colleen M. Niswender reports was provided by International Rett Syndrome Foundation. Rocco G. Gogliotti, Sheryl Anne D. Vermudez reports financial support was provided by National Institutes of Health. Kathrin Meyer, Cassandra Dennys has patent pending to Nationwide Children's Hospital. If there are other authors, they declare that they have no known

Fig. 6. Increasing Mecp2 levels leads to improvement in *Tcf4*^{+/-} pyramidal cell morphology.

Mice were treated as described in Fig. 5. (A–C) Representative images of dendrites from pyramidal cells from p120 *Tcf4*^{+/+}, *Tcf4*^{+/-} and *Tcf4*^{+/-}-scAAV9.P546.MeCP2-injected mice. When compared to the WT group, both treated and untreated *Tcf4*^{+/-} samples showed significant reductions in dendritic length (upper panel, A to C, Scale bar: 50 µm), the number of the dendritic spines, and overall spine density (boxes in the lower panel, A' to C'; Scale bar: 5 µm) compared to control. These observations were consistent for both basal and apical dendrites. Quantification of dendritic length (D–F), number of dendritic spines (G–I), and overall spine density (J–L) was performed using NeuroLucida (MBF Bioscience, VT). Importantly, treatment with AAV9.MECP2 significantly improved total dendrite length, spine counts and spine density overall and in both basal and apical dendrites. Statistical analysis was performed using One-way ANOVA with Tukey post-hoc analysis comparing the mean of each data set to the combined average of the controls (dotted line). *p < 0.05, **p < 0.01, ***p < 0.001, ****p < 0.0001.

competing financial interests or personal relationships that could have appeared to influence the work reported in this paper.

Acknowledgements

Funding was supported by a Basic Science Research grant from the International Rett Syndrome Foundation (CMN), R01 NS112171 (RGG), R21 HD111864 (RGG), generous grants from the Pitt Hopkins Research Foundation (CMN, KM, PC), and F31 MH119699 (to SADV). We would also like to thank the SCN2A foundation for the generous donation of the seahorse XE96 analyzer to Meyer lab, which was used to conduct the mitochondrial analysis. The following cell lines/DNA samples were obtained from the NIGMS Human Genetic Cell Repository at the Coriell Institute for Medical Research: [AG08620, GM26038, GM26091]. The remaining lines were collected from UCLA, Pamela Shaw, SiTranN, Sheffield UK and Jill Weimer, Sanford Research and TGEN.

Appendix A. Supplementary data

Supplementary data to this article can be found online at <https://doi.org/10.1016/j.neurot.2024.e00376>.

References

- Zweier C, Peippo MM, Hoyer J, Sousa S, Bottani A, Clayton-Smith J, et al. Haploinsufficiency of TCF4 causes syndromal mental retardation with intermittent hyperventilation (Pitt-Hopkins syndrome). *Am J Hum Genet* 2007;80(5).
- Sweeter DA, Elsharkawi I, Yonker L, Steeves M, Parkin K, Thibert R. Pitt-hopkins syndrome [Updated 2018 Apr 12]. In: Adam MP, Feldman J, Mirzaa GM, Pagon RA, Wallace SE, Bean LJH, editors. *GeneReviews®* [Internet]. Seattle (WA): University of Washington, Seattle; 2012 Aug 30. 1993-2024. Available from: <http://www.ncbi.nlm.nih.gov/books/NBK100240/>.
- Giurgea I, Missirian C, Cacciagli P, Whalen S, Fredriksen T, Gaillon T, et al. TCF4 deletions in Pitt-Hopkins syndrome. *Hum Mutat* 2008 Nov;29(11).
- Dong JY, Fan PD, Frizzell RA. Quantitative analysis of the packaging capacity of recombinant adeno-associated virus. *Hum Gene Ther* [Internet] 1996 Nov 10;7(17):2101–12 [cited 2023 Jun 21]. Available from: <https://pubmed.ncbi.nlm.nih.gov/8934224/>.
- Amir RE, Van Den Veyver IB, Wan M, Tran CQ, Francke U, Zoghbi HY. Rett syndrome is caused by mutations in X-linked MECP2, encoding methyl-CpG-binding protein 2. *Nat Genet* 1999 Oct;23(2):185–8.
- Ehrhart F, Coort SLM, Cirillo E, Smeets E, Evelo CT, Curfs LMG. Rett syndrome – biological pathways leading from MECP2 to disorder phenotypes. *Orphanet J Rare Dis* 2016;11(1):1–13. 11:1 [Internet]. 2016 Nov 25 [cited 2024 Jan 29]. Available from: <https://ojrd.biomedcentral.com/articles/10.1186/s13023-016-0545-5>.
- Tillotson R, Bird A. The molecular basis of MeCP2 function in the brain. *J Mol Biol* [Internet] 2020 Mar 13;432(6):1602–23 [cited 2024 Jan 29]; Available from: <http://pubmed.ncbi.nlm.nih.gov/31629770/>.
- Samaco RC, Neul JL. Complexities of Rett syndrome and MeCP2. *J Neurosci* [Internet] 2011 Jun 1;31(22):7951–9 [cited 2024 Jan 29]; Available from: <https://www.jneurosci.org/content/31/22/7951>.
- Liyanage VRB, Rastegar M. Rett syndrome and MeCP2. *NeuroMolecular Med* [Internet] 2014;16(2):231 [cited 2024 Jan 29]; Available from: <https://pubmed.ncbi.nlm.nih.gov/22383159/>.
- Dennys CN, Roussel F, Rodrigo R, Zhang X, Sierra Delgado A, Hartlaub A, et al. CuATSM effectively ameliorates ALS patient astrocyte-mediated motor neuron toxicity in human in vitro models of amyotrophic lateral sclerosis. *Glia* [Internet] 2023 Feb 1;71(2):350 [cited 2023 Jun 21]; Available from: <https://pubmed.ncbi.nlm.nih.gov/36297379/>.
- Sinha Ray S, Dutta D, Dennys C, Powers S, Roussel F, Lisowski P, et al. Mechanisms of IRF2BPL-related disorders and identification of a potential therapeutic strategy. *Cell Rep* [Internet] 2022 Dec 6;41(10) [cited 2023 Jun 21]; Available from: <http://www.cell.com/article/S2211124722016345/fulltext>.
- Meyer K, Ferraiuolo L, Miranda CJ, Likhite S, McElroy S, Renusch S, et al. Direct conversion of patient fibroblasts demonstrates non-cell autonomous toxicity of astrocytes to motor neurons in familial and sporadic ALS. *Proc Natl Acad Sci U S A* [Internet] 2014 Jan 1;111(2):829–32 [cited 2023 Jun 21]; Available from: <https://pubmed.ncbi.nlm.nih.gov/23896192/>.
- Dennys CN, Sierra-Delgado JA, Ray SS, Hartlaub AM, Roussel FS, Rodriguez Y, et al. In vitro modeling for neurological diseases using direct conversion from fibroblasts to neuronal progenitor cells and differentiation into astrocytes. *JoVE* [Internet] 2021 Jun 10;2021(172):e62016 [cited 2023 Jul 24]; Available from: <https://www.jove.com/v/62016/in-vitro-modeling-for-neurological-diseases-using-direct-con-ve>.
- Pilotto F, Schmitz A, Maharjan N, Diab R, Odriozola A, Tripathi P, et al. PolyGA targets the ER stress-adaptive response by impairing GRP75 function at the MAM in C9ORF72-ALS/FTD. *Acta Neuropathol* [Internet] 2022 Nov 1;144(5):939–66 [cited 2023 Jul 24]; Available from: <https://link.springer.com/article/10.1007/s00401-022-02494-5>.
- Gatto N, Dos Santos Souza C, Shaw AC, Bell SM, Myszczyńska MA, Powers S, et al. Directly converted astrocytes retain the ageing features of the donor fibroblasts and elucidate the astrocytic contribution to human CNS health and disease. *Aging Cell* [Internet] 2021 Jan 1;20(1):e13281 [cited 2023 Jul 24]; Available from: <https://onlinelibrary.wiley.com/doi/full/10.1111/ace1.13281>.
- Albizzati E, Florio E, Miramondi F, Sormonta I, Landsberger N, Frasca A. Identification of region-specific cytoskeletal and molecular alterations in astrocytes of MeCP2 deficient animals. *Front Neurosci* 2022 Feb 15;16:823060.
- Rakela B, Brehm P, Mandel G. Astrocytic modulation of excitatory synaptic signaling in a mouse model of Rett syndrome. *Elife* 2018 Jan 9;7.
- Dong Q, Liu Q, Li R, Wang A, Bu Q, Wang KH, et al. Mechanism and consequence of abnormal calcium homeostasis in Rett syndrome astrocytes. *Elife* [Internet] 2018 Mar 29;7 [cited 2023 Oct 11]; Available from: <https://pubmed.ncbi.nlm.nih.gov/30463906/>.
- Collins AL, Levenson JM, Vilaythong AP, Richman R, Armstrong DL, Noebels JL, et al. Mild overexpression of MeCP2 causes a progressive neurological disorder in mice. *Hum Mol Genet* [Internet] 2004 Nov 1;13(21):2679–89 [cited 2023 Oct 9]; Available from: <https://pubmed.ncbi.nlm.nih.gov/15351775/>.
- Heckman LD, Chahrouh MH, Zoghbi HY. Rett-causing mutations reveal two domains critical for MeCP2 function and for toxicity in MECP2 duplication syndrome mice. *Elife* 2014 Jun 26;2014(3).
- Lamonica JM, Kwon DY, Goffin D, Fenik P, Johnson BS, Cui Y, et al. Elevating expression of MeCP2 T158M rescues DNA binding and Rett syndrome-like phenotypes. *J Clin Invest* [Internet] 2017 May 1;127(5):1889–904 [cited 2023 May 1]; Available from: <https://pubmed.ncbi.nlm.nih.gov/28394263/>.
- Koerner MV, Fitzpatrick L, Selfridge J, Guy J, De Sousa D, Tillotson R, et al. Toxicity of overexpressed MeCP2 is independent of HDAC3 activity. *Genes Dev* [Internet] 2018 Dec 1;32(23–24):1514–24 [cited 2023 May 1]; Available from: <https://pubmed.ncbi.nlm.nih.gov/30463906/>.
- Collins BE, Merritt JK, Erickson KR, Neul JL. Safety and efficacy of genetic MECP2 supplementation in the R294X mouse model of Rett syndrome. *Genes Brain Behav* [Internet] 2022 Jan 1;21(1) [cited 2023 May 1]; Available from: <https://pubmed.ncbi.nlm.nih.gov/33942492/>.
- Vermudez SAD, Gogliotti RG, Arthur B, Buch A, Morales C, Moxley Y, et al. Profiling beneficial and potential adverse effects of MeCP2 overexpression in a hypomorphic Rett syndrome mouse model [*Genes Brain Behav* [Internet] 2022 Jan 1;21(1). cited 2023 May 1]; Available from: <https://pubmed.ncbi.nlm.nih.gov/34002468/>.
- Pitcher MR, Herrera JA, Buffington SA, Kochukov MY, Merritt JK, Fisher AR, et al. Rett syndrome like phenotypes in the R255X MeCP2 mutant mouse are rescued by MECP2 transgene. *Hum Mol Genet* [Internet] 2015 May 1;24(9):2662–72. <https://doi.org/10.1093/hmg/ddv030> [cited 2023 Jun 21]; Available from: .
- Kennedy AJ, Rahn EJ, Paulukaitis BS, Savell KE, Kordasiewicz HB, Wang J, et al. Tcf4 regulates synaptic plasticity, DNA methylation, and memory function. *Cell Rep* 2016 Sep 1;16(10):2666–85.
- Seibenhener ML, Wooten MC. Use of the open field maze to measure locomotor and anxiety-like behavior in mice. *J Visual Exper* 2015 Feb 6;(96).
- Meyer K, Ferraiuolo L, Schmelzer L, Braun L, McGovern V, Likhite S, et al. Improving single injection CSF delivery of AAV9-mediated gene therapy for SMA: a dose–response study in mice and nonhuman primates. *Mol Ther* [Internet] 2015 Mar 5;23(3):477 [cited 2024 Jan 25]; Available from: <https://pubmed.ncbi.nlm.nih.gov/254351452/>.
- Johnson TB, Brudvig JJ, Likhite S, Pratt MA, White KA, Cain JT, et al. Early postnatal administration of an AAV9 gene therapy is safe and efficacious in CLN3 disease. *Front Genet* [Internet] 2023;14 [cited 2024 Jan 25]; Available from: <https://pubmed.ncbi.nlm.nih.gov/36297379/>.
- Johnson TB, White KA, Brudvig JJ, Cain JT, Langin L, Pratt MA, et al. AAV9 gene therapy increases lifespan and treats pathological and behavioral abnormalities in a mouse model of CLN8-batten disease [*Mol Ther* [Internet] 2021 Jan 1;29(1):162. cited 2024 Jan 25]; Available from: <https://pubmed.ncbi.nlm.nih.gov/33942492/>.
- Cain JT, Likhite S, White KA, Timm DJ, Davis SS, Johnson TB, et al. Gene therapy corrects brain and behavioral pathologies in CLN6-batten disease. *Mol Ther* [Internet] 2019 Oct 10;27(10):1836 [cited 2024 Jan 25]; Available from: <https://pubmed.ncbi.nlm.nih.gov/31629770/>.
- Powers S, Likhite S, Gadalla KK, Miranda CJ, Hufferberger AJ, Dennys C, et al. Novel MECP2 gene therapy is effective in a multicenter study using two mouse models of Rett syndrome and is safe in non-human primates. *Mol Ther* [Internet] 2023 Sep 6;31(9):2767–82 [cited 2023 Sep 29]; Available from: <http://www.cell.com/article/S1525001623003933/fulltext>.
- Deacon RMJ, Rawlins JNP. Hippocampal lesions, species-typical behaviours and anxiety in mice. *Behav Brain Res* [Internet] 2005 Jan 30;156(2):241–9 [cited 2023 Jun 21]; Available from: <https://pubmed.ncbi.nlm.nih.gov/15582110/>.
- Armani R, Archer H, Clarke A, Vasudevan P, Zweier C, Ho G, et al. Transcription factor 4 and myocyte enhancer factor 2C mutations are not common causes of Rett syndrome. *Am J Med Genet A* [Internet] 2012 Apr;158A(4):713–9 [cited 2023 Jul 25]; Available from: <https://pubmed.ncbi.nlm.nih.gov/22383159/>.
- Vidal S, Xiol C, Pascual-alonso A, O'callaghan M, Pineda M, Armstrong J. Genetic landscape of Rett syndrome spectrum: improvements and challenges. *Int J Mol Sci* 2019;20(16):3925. Vol 20, Page 3925 [Internet]. 2019 Aug 12 [cited 2023 Jul 25]; Available from: <https://www.mdpi.com/1422-0067/20/16/3925/html>.
- Pejhan S, Del Bigio MR, Rastegar M. The MeCP2E1/E2-BDNF-miR132 homeostasis regulatory network is region-dependent in the human brain and is impaired in Rett syndrome patients. *Front Cell Dev Biol* [Internet] 2020 Aug 21;8 [cited 2024 Jan 29]; Available from: <https://pubmed.ncbi.nlm.nih.gov/33942492/>.
- Smrt RD, Pfeiffer RL, Zhao X. Age-dependent expression of MeCP2 in a heterozygous mosaic mouse model [*Hum Mol Genet* [Internet] 2011 May 5;20(9):1834. cited 2024 Jan 29]; Available from: <https://pubmed.ncbi.nlm.nih.gov/201401674/>.

- [38] Kim JJ, Savas JN, Miller MT, Hu X, Carroumeu C, Lavallée-Adam M, et al. Proteomic analyses reveal misregulation of LIN28 expression and delayed timing of glial differentiation in human iPS cells with MECP2 loss-of-function. *PLoS One* [Internet] 2019 Feb 1;14(2):e0212553 [cited 2023 Jul 25]; Available from: <https://journals.plos.org/plosone/article?id=10.1371/journal.pone.0212553>.
- [39] Papes F, Camargo AP, de Souza JS, Carvalho VMA, Szeto RA, LaMontagne E, et al. Transcription Factor 4 loss-of-function is associated with deficits in progenitor proliferation and cortical neuron content. *Nat Commun* 2022;13(1):1–26. 13:1 [Internet]. 2022 May 2 [cited 2023 Jul 25]; Available from: <https://www.nature.com/articles/s41467-022-29942-w>.
- [40] Shariq M, Sahasrabudde V, Krishna S, Radha S, Nruthyathi, Bellampalli R, et al. Adult neural stem cells have latent inflammatory potential that is kept suppressed by Tcf4 to facilitate adult neurogenesis. *Sci Adv* [Internet] 2021 May 1;7(21):5606–27 [cited 2023 Jul 25]; Available from: <https://pmc/articles/PMC8139598/>.
- [41] Bedogni F, Gigli CC, Pozzi D, Rossi RL, Scaramuzza L, Rossetti G, et al. Defects during Mecp2 null embryonic cortex development precede the onset of overt neurological symptoms. *Cereb Cortex* [Internet] 2016 Jun 1;26(6):2517–29 [cited 2024 Jan 29]; Available from: <https://pubmed.ncbi.nlm.nih.gov/25979088/>.
- [42] Squillaro T, Alessio N, Cipollaro M, Melone MAB, Hayek G, Renieri A, et al. Reduced expression of MECP2 affects cell commitment and maintenance in neurons by triggering senescence: new perspective for Rett syndrome. *Mol Biol Cell* [Internet] 2012 Apr 15;23(8):1435–45 [cited 2024 Jan 29]; Available from: <https://pubmed.ncbi.nlm.nih.gov/22357617/>.
- [43] Andoh-Noda T, Akamatsu W, Miyake K, Matsumoto T, Yamaguchi R, Sanosaka T, et al. Differentiation of multipotent neural stem cells derived from Rett syndrome patients is biased toward the astrocytic lineage. *Mol Brain* [Internet] 2015 May 27;8(1):1–11 [cited 2024 Jan 29]; Available from: <https://molecularbrain.biomedcentral.com/articles/10.1186/s13041-015-0121-2>.
- [44] Alessio N, Riccitiello F, Squillaro T, Capasso S, Del Gaudio S, Di Bernardo G, et al. Neural stem cells from a mouse model of Rett syndrome are prone to senescence, show reduced capacity to cope with genotoxic stress, and are impaired in the differentiation process. *Exp Mol Med* 2018;50(3):1–9. 50:3 [Internet]. 2018 Mar 22 [cited 2024 Jan 29]; Available from: <https://www.nature.com/articles/s12276-017-0005-x>.
- [45] Feldman D, Banerjee A, Sur M. Developmental dynamics of Rett syndrome. *Neural Plast* 2016;2016 [cited 2024 Jan 29]; Available from: <https://pmc/articles/PMC4752981/>.
- [46] Gadalla KKE, Vudhironarit T, Hector RD, Sinnett S, Bahey NG, Bailey MES, et al. Development of a novel AAV gene therapy cassette with improved safety features and efficacy in a mouse model of Rett syndrome. *Mol Ther Methods Clin Dev* [Internet] 2017 Jun 6;5:180 [cited 2024 Jan 29]; Available from: <https://pmc/articles/PMC5423329/>.
- [47] Sinnett SE, Boyle E, Lyons C, Gray SJ. Engineered microRNA-based regulatory element permits safe high-dose miniMECP2 gene therapy in Rett mice. *Brain* [Internet] 2021 Oct 1;144(10):3005 [cited 2024 Jan 29]; Available from: <https://pmc/articles/PMC8783608/>.
- [48] Koerner MV, Fitzpatrick L, Selfridge J, Guy J, De Sousa D, Tillotson R, et al. Toxicity of overexpressed MeCP2 is independent of HDAC3 activity. *Genes Dev* [Internet] 2018 Dec 1;32(23–24):1514–24 [cited 2023 Oct 11]; Available from: <http://genesdev.cshlp.org/content/32/23-24/1514.full>.
- [49] Sandweiss AJ, Brandt VL, Zoghbi HY. Advances in understanding of Rett syndrome and MECP2 duplication syndrome: prospects for future therapies. *Lancet Neurol* [Internet] 2020 Aug 1;19(8):689–98 [cited 2023 Oct 11]; Available from: <http://www.thelancet.com/article/S1474442220302179/fulltext>.
- [50] Sanderson DJ, Cunningham C, Deacon RMJ, Bannerman DM, Perry VH, Rawlins JNP. A double dissociation between the effects of sub-pyrogenic systemic inflammation and hippocampal lesions on learning. *Behav Brain Res* [Internet] 2009 Jul 19;201(1):103–11 [cited 2023 Jun 21]; Available from: <https://pubmed.ncbi.nlm.nih.gov/19428623/>.
- [51] Sanderson DJ, Rawlins JNP, Deacon RMJ, Cunningham C, Barkus C, Bannerman DM. Hippocampal lesions can enhance discrimination learning despite normal sensitivity to interference from incidental information. *Hippocampus* [Internet] 2012 Jul;22(7):1553–66 [cited 2023 Jun 21]; Available from: <https://pubmed.ncbi.nlm.nih.gov/22161993/>.
- [52] Deacon RMJ. Assessing nest building in mice. *Nat Protoc* [Internet] 2006 Aug;1(3):1117–9 [cited 2023 Jun 21]; Available from: <https://pubmed.ncbi.nlm.nih.gov/17406392/>.
- [53] Deacon R, Altimiras F, Bazan-Leon E, Pyarasani R, Nachtigall F, Santos L, et al. Natural AD-like neuropathology in Octodon degus: impaired burrowing and neuroinflammation. *Curr Alzheimer Res* 2015 May 1;12(4):314–22.
- [54] Sierra-Delgado JA, Likhite S, Bautista PK, Gómez-Ochoa SA, Echeverría LE, Guío E, et al. Prevalence of neutralizing antibodies against adeno-associated virus serotypes 1, 2, and 9 in non-injected Latin American patients with heart failure-ANVIAS study. *Int J Mol Sci* [Internet] 2023 Mar 14;24(6):5579 [cited 2023 Jun 26]; Available from: <https://pubmed.ncbi.nlm.nih.gov/36982654/>.
- [55] Hunsaker MR, Fieldsted PM, Rosenberg JS, Kesner RP. Dissociating the roles of dorsal and ventral CA1 for the temporal processing of spatial locations, visual objects, and odors. *Behav Neurosci* 2008 Jun;122(3):643–50.
- [56] Hoge J, Kesner RP. Role of CA3 and CA1 subregions of the dorsal hippocampus on temporal processing of objects. *Neurobiol Learn Mem* [Internet] 2007 Sep;88(2):225–31 [cited 2023 Jul 25]; Available from: <https://pubmed.ncbi.nlm.nih.gov/17560815/>.
- [57] Hunsaker MR. The importance of considering all attributes of memory in behavioral endophenotyping of mouse models of genetic disease. *Behav Neurosci* [Internet] 2012 Jun;126(3):371 [cited 2023 Jul 25]; Available from: <https://pmc/articles/PMC3367383/>.